Effects of Vertical Motions on Seismic Response of Goltzschtal Masonry Arch Bridge

Mirhasan Moosavi[1], Mansour Ziyaeifar[2], Masoud Nekooei[3], and Javad Mokari[4]*

1. Ph.D. Student, Department of Civil Engineering, Science and Research Branch, Islamic Azad University, Tehran, Iran, * Corresponding Author; email: mh_moosavi@iausalmas.ac.ir
2. Associate Professor, Structural Engineering Research Center, International Institute of Earthquake Engineering and Seismology (IIEES), Tehran, Iran
3. Assistant Professor, Department of Civil Engineering, Science and Research Branch, Islamic Azad University, Tehran, Iran
4. Assistant Professor, Urmia University and Technology, Urmia, Iran

Received: 01/10/2015
Accepted: 15/03/2016

ABSTRACT

Previous researches have demonstrated that the effects of earthquake vertical component on main structural elements of bridges are very noticeable in near-fault seismic events. In the near distances of seismic source (D<10 to 15 km) the response spectrum of a vertical component has a great peak in short-period regions. Owing to geometrical shape and mechanical properties, masonry arch bridges have lower characteristic periods. It seems that, in this type of bridge, axial force response is considerable under vertical seismic events. In this article, a simple analytic model for masonry arch bridges is introduced. Vertical motions effects on seismic axial force response of masonry arch bridges are investigated through dynamic time history analysis of the world's largest masonry arch bridge simplified model. Vertical component effects on bridge structural elements are measured using a ratio computed by dividing the average values resulted from time history analysis based on applying three components of earthquakes simultaneously for seven selected records to responses of dead load applying. Then, the bridge's simplified model dynamic analysis results are verified by the results obtained from accurate finite element model dynamic analysis. Besides, in order to investigate the effects of low tension strength of masonry materials, the results obtained from nonlinear dynamic analysis in which tension strength of material is assumed to be zero, are compared with those obtained from linear dynamic analysis. This survey shows that vertical component effects in some structural elements of bridges are very considerable.

Keywords:
Vertical component;
Seismic design;
Goltzschtal Bridge;
Masonry arch bridges;
Dynamic analysis

1. Introduction

Many bridge engineers assume that vertical ground motions during seismic events are unimportant. Vertical components of earthquakes have unique properties that make it distinct from horizontal components. For vertical motions, recent observations suggest that the commonly adopted vertical to horizontal response spectral ratio of (2/3) [1] may be significantly increased at short-period regions in the near-source distances [2]. Most bridges design analyses performed on bridges are linear elastic models using response spectrum method. Bridge design codes have not provided load multipliers or specific vertical response spectra that allow to include the impact of the vertical motions rationally. Linear elastic analyses of bridges demonstrate that bridges with great percent of modal mass associated

with periods near the maximum amplitude of vertical response spectrum experience the greatest effects from vertical seismic motions. Thus, for some force response quantities of such bridges, response from dead loading must be multiplied by 2 to account the effect of vertical motions [3].

The first major analytical study into the effects of vertical acceleration on bridges was completed by Saadeghvaziri and Foutch [4]. They reported that San Fernando's vertical peak acceleration in Pacoima dam station was 0.7g and fault peak displacement was 6 ft in vertical direction. Peak acceleration in Elasnam earthquake (1980) was estimated to be 1g in vertical direction and 0.25g in horizontal direction. A finite element code capable of modelling the inelastic behaviour of reinforced concrete columns under combined horizontal and vertical deformations was used. With three-dimensional finite element modelling of eight bridges, they demonstrated that axial force variation in the columns results in pinched hysteresis causes larger horizontal displacements and fluctuation in columns shear capacity. The study result showed that for earthquake motions with effective peak acceleration (EPA) of 0.4g or less, the additional damage caused by the vertical component was minimal, while for earthquakes motions with EPA of 0.7g, the addition of the vertical component resulted in considerably more damage [4].

Parametric studies into the effects of vertical acceleration on bridges were conducted by Yu et al. [5], Broekhuizen [6], and Yu [7]. All studies centralized on three overpasses of the SR14/15 interchange location about 15 km north of the epicentre of the 1994 Northridge earthquake. Two of these bridges were partially collapsed during that earthquake [5]. An investigation on the effects of vertical acceleration on pre-stressed concrete bridges was carried out by Broekhuizen [6]. He assumed 1g upward acceleration, and found that allowable tensile stresses in deck could be exceeded [6]. Yu et al. [5] and Yu [7] by using 3D linear models with Sylmar hospital (Northridge) record as an input motion, analysed forces in all piers of three overpasses. The study found a 21% increase in axial force and a 7% change in longitudinal moment due to the addition of the vertical component. Yu [7] considered the effects of the vertical earthquake motions on bridge foundations, hinges and bearings. In this study, soil stiffness was varied for spread footing and friction-pile foundation. The maximum response was found to be increased as the shear-wave velocity of the soil increased, approaching the limiting values obtained assuming rigid base. The presentation criteria used in the design of 60 pre-stressed box-girder bridges in which the effects of vertical ground motion were considered, carried out by Yu [7] and Gloyd [8]. Li et al. [9] demonstrated that the vertical component effects on highway bridges with low periods were great. Kunnath et al. [10] showed the variation of axial loads effects due to vertical components on ordinary highway bridges and presented that vertical acceleration could considerably increase tension stresses in deck and decrease flexural and shear capacity in piers.

Hosseinzadeh [11] studied the effects of vertical components on reinforced concrete piers of bridges. He selected two concrete pier of a bridge and analyzed piers under Tabas earthquake record with various horizontal PGA and 50% of horizontal PGA as vertical component PGA. He found that applying vertical component, increased the cracks widths of 60% and changed cracking mechanism from flexural to shearing.

Few studies can be found concerning seismic performances of masonry bridges. Armstrong [12] evaluated dynamic properties of two stone bridges by field studies. Brencich et al. [13] measured dynamic properties of a multi-span masonry bridge and compared the results with those obtained from the finite-element modelling. Bayraktar et al. [14] modelled a two-span masonry bridge analytically based on the results obtained from modal tests and updated the analytical model. Caglayan et al. [15] calibrated two masonry arch bridges based on the results obtained from ambient vibration test and the finite element modelling and calculated seismic response of bridges. Yazdani and Marefat [16] estimated damping ratios for two unreinforced concrete arch bridge based on modal properties resulted from the vibration test and the finite element modelling. Pela et al. [17] studied the effectiveness of non-linear static analysis methods for evaluation of seismic performance for a three-arched masonry arch bridge based on comparison responses obtained from nonlinear static analysis method with those obtained from the nonlinear dynamic analysis method.

These studies show that because of geometrical shape and mechanical properties, masonry arch bridges have low characteristic periods and large amount of bridges modal mass is concentrated on low-period regions. Consequently, such bridges can be very sensitive to vertical component of earthquakes. On the other hand, these historical bridges, the oldest railway infrastructure elements in existence, still serve as a major component of these systems in many countries. Masonry arch bridges are an integral component of the heritage of cultures worldwide and their preservation is of the utmost importance. Moreover, a significant number is being used for motorized traffic currently. It is the utmost importance to insure the safety of these historical bridges against the dynamic loading of traffic, wind and earthquakes. Literature shows that finite element-based methods and arc concepts are usual methods for the analysis of such bridges against dynamic loads. These methods are the most expensive ones, and geometrical and material models that are used are so complicated. Thus, for simplification of studying linear and nonlinear behaviours of such structures, the representation of a simple analytic model is essential. By studying the effects of dynamic loads on various simplified model elements, it is possible to redraw a new geometry for masonry bridges in which load effects are minimized and since neither of the above-mentioned studies have not considered the effects of earthquakes vertical motions on masonry arch bridges, analysing and considering masonry bridges for such motions through a simple model seems to be essential.

2. Earthquake Vertical Component and Bridge Design Codes

In this part of article, the viewpoints of various design codes about vertical component of ground motions are represented. The Design codes that have been reviewed in this study are: Iranian Codes for Seismic Design of Roads and Railways Bridges [18], CALTRANS [19], Euro Code [20], AASHTO LRFD Bridge Design Specifications [21], AASHTO [22], AASHTO Seismic Isolation Guide Specifications [23], ASCE [24], IBC2012 [25] and UBC97 [26].

Iranian Codes for Seismic Design of Roads and Railway Bridges [18] considers only horizontal components and ignoring vertical component effects; recommends only the amount of design forces for deck support bolts. Caltrans applies a vertical load in ordinary and standard bridges that their site PGA exceeds 0.6 g and recommends the site study for evaluation of vertical component effects in important and complicated bridges. In the bridges with above-mentioned conditions, a uniform vertical load equivalent to one-fourth of the deck dead load is applied to the deck in upward and downward directions as shown in Figure (1) [19].

EuroCode 8 considers vertical earthquake motion effects explicitly during design procedure and offers vertical response spectrum for different soil types. Figures (2) and (3) show Type I and Type II response spectrum for vertical and horizontal components according to EuroCode 8 [20].

AASHTO does not have a direct method for applying vertical component on bridges, but instead AASHTO Seismic Isolation guide specifications [23] uses ±20% of dead load (i.e. load factors of 1.2 and 0.8) in the testing requirements to represent vertical effects, irrespective of earthquake magnitude, fault distance and soil type [21].

AASHTO LRFD Bridge Design Specifications [21] denotes for short-period motions in the near-fault

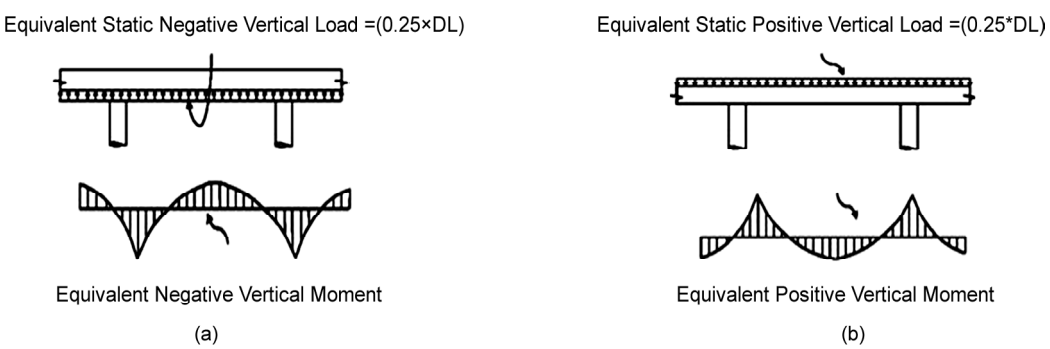

Figure 1. Upward and downward equivalent static loads and moments (Caltrans).

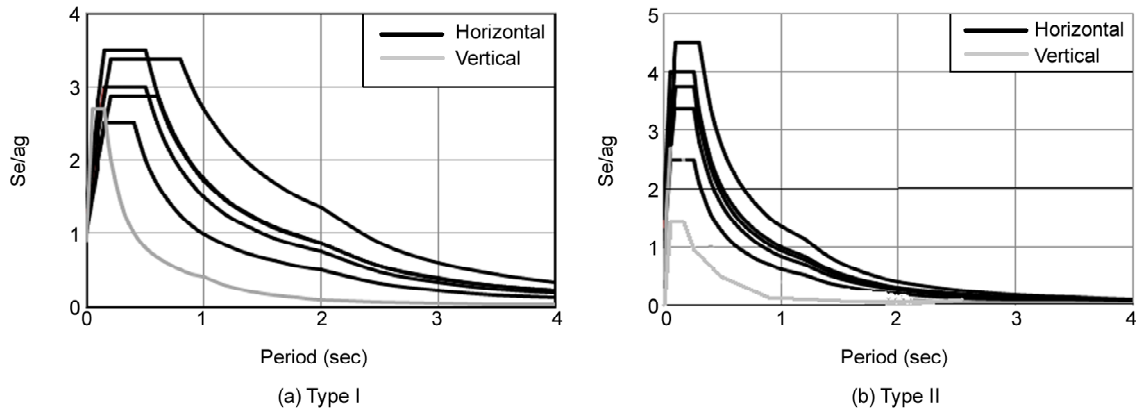

Figure 2. Response spectrum for vertical and horizontal components (Euro Code8).

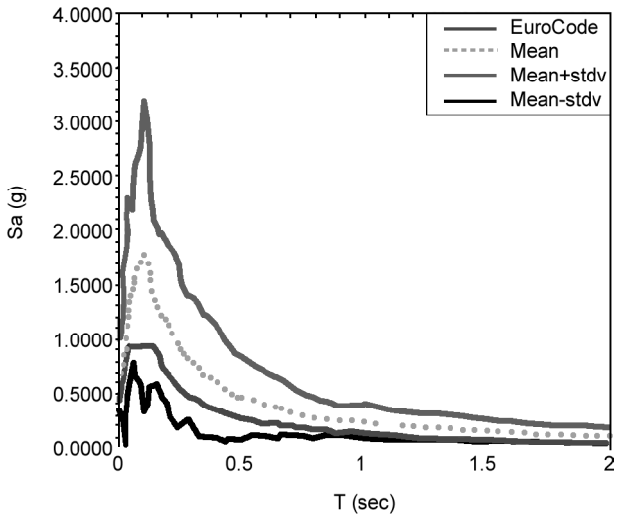

Figure 3. Vertical component response spectrum.

environment that the ratio of vertical to horizontal ground motions increase if the site is located within six miles of an active fault, intermediate to long periods ground motion pulses that are characteristics of the near-source time histories, should be included if these types of ground motion characteristics could significantly influence structural response. Similarly, the high short-period spectral content of near-source vertical ground motions should be considered.

IBC2012 denotes every structure and portion thereof, including non-structural components that are permanently attached to structure, their supports and attachments should be designed and constructed to resist the effects of earthquake motions in accordance with ASCE 7 and do not represent any independent instruction about vertical component effects [25].

In UBC 97 [26], structures should be designed for ground motion producing structural responses and seismic forces in any horizontal directions, the following earthquake loads ought to be used in load combination:

$$E = \rho.E_h + E_v \quad (1)$$

where E is the earthquake load on an element of structure resulted from the combination of horizontal component E_h, and the vertical component E_v. E_v is the load effect resulted from vertical component of earthquake ground motion and is equal to an addition of $0.5\,.\,C_a\,.\,I.\,D$ to dead load effect, D is for strength design and may be taken to zero for allowable stress design. Maximum value of $0.5.C_a.I$ product, according to tables represented in code is 81%. The vertical component of ground motion may be defined by scaling corresponding horizontal acceleration by a factor of two-thirds. Alternative factors may be used when substantiated by site specific data. Where the near source factor, N_a is greater than 1, site specific vertical response spectrum shall be used in lieu of the factor of two-thirds [26].

In ASCE7-10 [24] vertical seismic load effect E_v shall be determined in accordance with the following equation:

$$E_v = 0.2 S_{DS}.D \quad (2)$$

where S_{DS} is the design spectral response acceleration parameter at short periods and D is the effect of dead load [24].

In later stage of this study, a database consists of 31 near-fault earthquake records is gathered. The selected database consists of 61 horizontal and 31 vertical components of 31 worldwide earthquakes (reported by PEER-NGA database). Table (1)

Table 1. Specifications of 31 ground motions.

Earthquake Name	Station Name	PGA (g)	PGV (inch/sec)	PGD (inch)	Mag	Displacement (mil)
Baja California	Cerro Prieto	1.26	21.96	3.83	5.5	2.29
Cape Mendocino	Cape Mendicono	1.3	34.81	10.62	7.01	4.32
Chi-Chi Taiwan	Chy080	0.82	34.33	11.02	7.62	1.67
Chi-Chi Taiwan	Tcu071	0.62	23.89	15.20	7.62	3.3
Chi-Chi Taiwan-06	Tcu080	0.58	11.18	1.91	6.30	6.34
Coalinga-01	Pleasant Valley pp	0.57	17.75	2.71	6.36	5.23
Gazli, USSR	Karakyr	0.65	24.43	8.41	6.8	3.39
Imperial Valley-06	Bonds Corner	0.68	21.15	5.05	6.53	1.67
Imperial Valley-06	El Centro Array #8	0.54	22.36	12.99	6.53	2.40
Landers	Lucerne	0.73	42.83	74.94	7.28	1.36
Loma Prieta	Corralitos	0.52	16.35	4.17	6.93	2.39
Loma Prieta	Lgpc	0.78	30.37	16.8	6.93	2.41
Northridge-01	Pacoimadam (up le)	1.4	31.11	5.55	6.69	4.36
Northridge-01	Rinaldi Receiving	0.63	43.01	11.13	6.69	4.04
Northridge-01	Tarzana-Cedar Hill	1.67	37.68	13.5	6.69	9.69
San Fernando	Pacoima Dam up le	1.23	34.62	10.15	6.61	1.12
San Salvador	Geotech Investing	0.65	18.65	4.7	5.8	3.91
Imperial Valley-06	Agragias	0.29	13.33	3.73	6.53	0.4
Imperial Valley-06	El Centro Dif-Array	0.43	21.78	13.01	6.53	3.16
Imperial Valley-06	El Centro Array #6	0.43	32.73	17.69	6.53	0.84
Imperial Valley-06	El Centro Array #7	0.42	31.57	16.15	6.53	0.35
Loma Prieta	Capitola	0.48	13.59	2.81	6.93	9.46
Mammoth Lakes 01	Convict Creek	0.43	9.55	1.99	6.06	4.12
Morgan Hill	Gilroy Array #2	0.19	3.37	0.68	6.19	8.51
Morgan Hill	Gilroy Array #3	0.19	4.95	1.12	6.19	8.09
Morgan Hill	Gilroy Array #4	0.28	6.65	1.42	6.19	7.17
Northridge-01	Arleta-Nordhof-fi-st	0.33	12.11	5.02	6.69	5.37
Superstition Hills-02	WildLiquef.Array	0.19	12.68	8.11	6.54	14.82
Tabas	Tabas	0.688	17.95	6.71	7.40	
Bam	Bam	0.88	36.82	11.12	6.6	
Manjil	Abbar	0.58	15	4.17	7.7	

presents specifications of 31 selected ground motions.

The selected records have very close distance to faults and great magnitudes. Then, individual and mean and mean ± standard deviation response spectrum have been plotted for selected 31 earthquakes.

Figure (3) shows mean and mean ± standard deviation response spectrum for vertical component and response spectrum according to EuroCode 8. Figure (3) shows that mean spectrum of 31 records is approximately two times as great as that of Euro Code's spectrum in short period regions. Thus, usual assumption is that vertical component spectrum equal to 2/3 horizontal spectrum is not correct in short-period regions. Figures (4) and (5) show mean and mean ± standard deviation horizontal response spectrum for parallel and normal directions to fault prolongation respectively and response spectrum according to Iranian Code of 2800 for Type II soils.

The plots in Figures (4) and (5) are relatively similar, and spectrums differences are not noticeable.

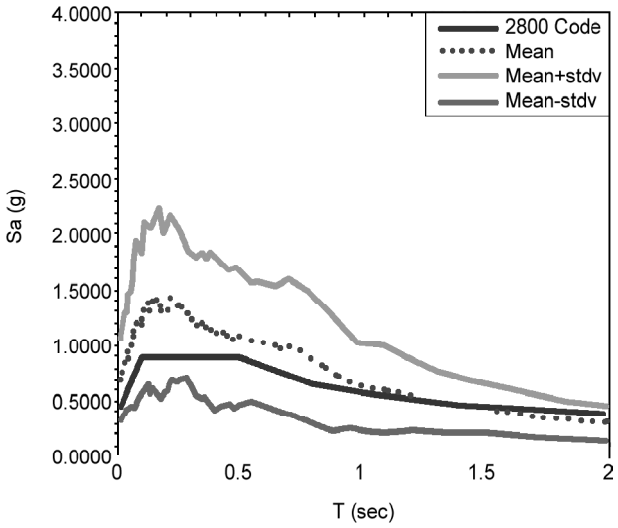

Figure 4. Horizontal fault parallel response spectrum.

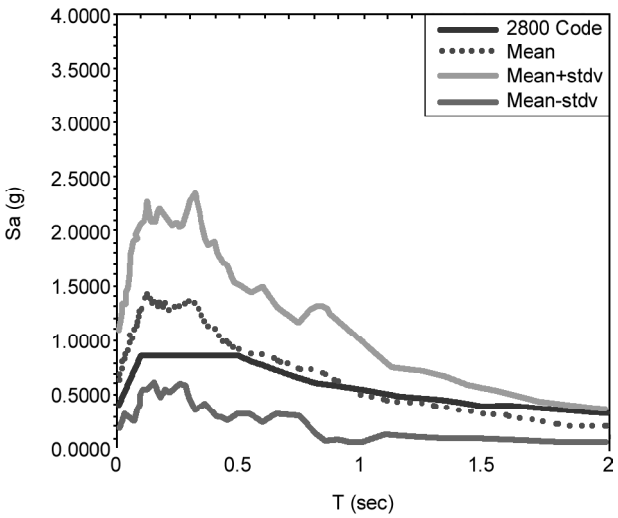

Figure 5. Horizontal fault normal response spectrum.

In contrast, in Figure (3), the spectrum plots differ dramatically.

3. Dynamic Properties of Masonry Arch Bridges

The studies show that conventional assumption of 5% for damping ratio in masonry arch bridges is overestimated, and using 3% damping ratio for horizontal modes and 1.5% for vertical modes is almost near to reality.

4. Masonry Arch Bridge's Simplified Model

Generally, for structural analysis simplification, mass, damping and stiffness are lumped in special joints of structure, and movement and deformation equations are solved in finite and discrete points of structure. This method simplifies the solution of problems and substantially some equations are solved exclusively by using this method. The position and number of discrete points depend on the geometry of structure, distribution of stiffness, damping and mass, load distribution and required accuracy. For example, in framed and truss structures subjected by static loads, discrete points are located in intersection of element's axes. Geometrical specification, type and amount of loads, internal forces and internal moments obtained from static and dynamic structural analysis and dynamic specification must be equal in real masonry arch bridge and simplified model. Since masonry materials do not have considerable tension resistance, external loads mostly produce compression internal forces in structural elements. Therefore, the selection of simplified model must be done in a manner that only compression forces are mostly produced in structural elements during external loading. It seems that among different types of structures, 2D frames with sloped ceiling, approximately have simple geometrical form and former mentioned specifications, thus arch is replaced by two linear elements that connect footing of arch to its head. Besides, internal forces level must be equal in real and simple model. Because axial internal force is varied along the arch, the average value of axial forces is used a criterion for conforming two models. Structural and nonstructural mass must be lumped in nodal points of frame. In circular arches, based on arches form and subjected loads, internal axial force is minimum on the top of arch and is maximum in its footing. The average value can be easily calculated by means of simple finite element modelling or simple integration. The results of many studies show that if 35% of total mass are lumped in the head of slopes and the remaining 65% are lumped in the footing of arch, the axial internal force level in inclined elements of simple 2D frame will be in the neighbourhood but a little less than the average value in real arch.

Besides, 50% of column's total mass are lumped on two ends of columns. The concentration of mass causes an increase in height of mass centre and the first mode period that frequently occurs in a direction perpendicular to bridge surface. Moreover, an increase in bridge vertical stiffness causes a decrease in period of the first vertical vibration mode. The decrease of inclined elements declination angle (angle between elements and horizontal extension) increases the axial internal force and inversely decreases the first horizontal and vertical natural period, resulting in the equality of key parameters in real and simple model. Furthermore, it is worth noting that all nodes settled on road-way's level are restrained in bridge longitudinal direction for modelling high axial stiffness of longitudinal elements and deck both ends connections to side's solid supports. Figures (6) and (7) show a single span arch bridge and its simplified model respectively.

5. Goltzschtal Bridge

5.1. Location And Geometry

The Goltzsch viaduct (in German: Goltzschtal

bruke) is a railway bridge in Germany. It is the largest brick bridge in the world, and for some time it was also the tallest railway bridge in the world.

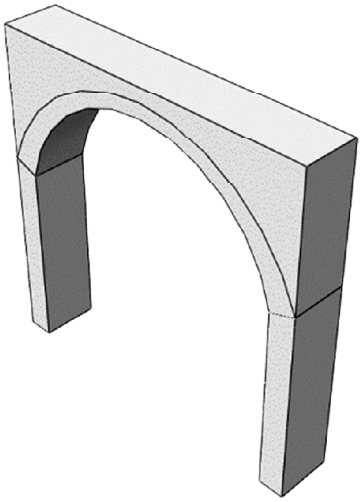

Figure 6. Single span arch bridge.

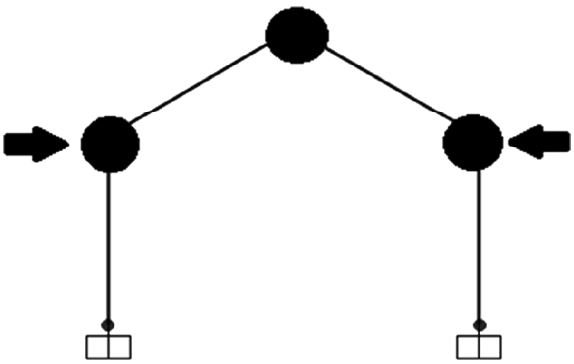

Figure 7. Single span arch bridge simplified model.

It spans the valley of the Goltzsch River between Mylau and Netzschkau, around 4 km west of Reichenbach im Vogtland in the German free state of Saxony. It was built between 1846 and 1851 as part of the railway between Saxony (Leipzig, Zwickau and Plauen) and Bavaria (Hof and Nuremberg). It is currently part of the Leipzig-Hof line, near the Netzschkau station. About 10 km south, the smaller Elster viaduct was built for the same line that was quite similar to the Goltzsch viaduct and named "little sister". Table (2) presents other specifications and Figure (8) shows a view of Goltzschtal Bridge [27].

Similar to what mentioned in section 5, a simplified model of Goltzschtal Bridge is built and the effects of earthquake vertical component are considered on various elements of model (Figure 9).

Figure 8. A view of Goltzschtal bridge.

Table 2. Specifications of Goltzschtal Bridge (Wikipedia, the free Encyelopaedia, Gultzsch Viaduct).

Carries: Two Railway Tracks	Crosses: Goltzsch river
Locate: Netzschkau, Saxony, Germany	Designer: John Andreas Schubert
Design: Arch Bridge	Material: Brick
Total Length: 574 m	Width: 23 m at Foot 9 m at Top
Height: 78 m	Number of Spans: 98 Vaults at 4 Level
Construction Begin: 31 May 1846	Construction End: 1851
Construction Cost: 2.2 Million Thalers	Opened: 15 July 1851

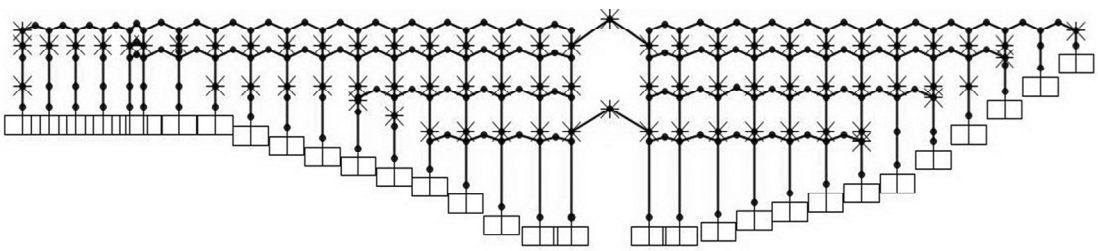

Figure 9. Simplified model of Goltzschtal Bridge.

5.2. Nonlinear Time History Analysis of Goltzschtal Bridge

Direct integration time history analysis has been used for dynamic analysis of Goltzschtal Bridge. Time history dynamic analysis of the model is carried out by seven scaled records and applying all three components of each earthquake simultaneously. Records are selected from 30 candidates listed in Table (1). Scaling is done in a manner that %5 damped response spectrum of each record is compatible with code's 5% damped spectrum according to EuroCode 8 provisions. Table (3) shows seven selected records for time history analysis and relevant scaling factors for horizontal and vertical components according to EuroCode 8 [20].

Table 3. Scaling factors for seven selected records.

Earthquake Name	Scaling Factor	
	Vertical	Horizontal
Tabas-Tabas	1.105	0.88
Bam-Bam	1.03	1.39
Manjil-Abbar	1.09	1.59
Gazli-Karakyr	0.62	1.20
Imperial Valley	0.72	1.88
Northridge	0.92	0.78
San Fernando	1.04	1.08

The effects of vertical components on Goltzschtal Bridge structural elements are measured using a ratio that is computed by dividing the average values resulted from time history analysis based on applying three components of earthquakes simultaneously for seven selected records to the dead load response of the elements and presented as $\frac{EQ}{DL}$. The average values for $\frac{EQ}{DL}$ ratio for pier axial forces, axial forces of minor arches and two major arch in all stories of the bridge are demonstrated in Table (4). For further investigation on the distribution of minor arches axial forces in various stories of bridge, two different bays of the bridge are selected and variation of axial forces in various stories of selected bays are reviewed in Table (5). One of two selected bays is located near the bridge central axes and the other one is selected far from central axes of the bridge.

Table 4. Average value of $\frac{EQ}{DL}$ for key structural elements.

Story	Average Value of $\frac{EQ}{DL}$		
	Pier's Axial Forces	Minor Arches Axial Forces	Major Arches Axial Forces
1	2.57	9.16	5.19
2	2.67	7.46	
3	3.32	8.11	7.52
4	3.61	6.23	

Table 5. Average value of $\frac{EQ}{DL}$ for arches axial forces.

Story	Average Value of $\frac{EQ}{DL}$	
	Close to Bridge Axe's	Far from Bridge Axe's
1	7.66	11.58
2	9.02	5.5
3	10.82	6.6
4	10.94	5.34

6. Verification

For verification of the simplified model dynamic analysis results, Goltzschtal Bridge accurate finite element model is created in ABAQUS software environment. Figure (10) shows a view of Goltzschtal Bridge accurate finite element model [28].

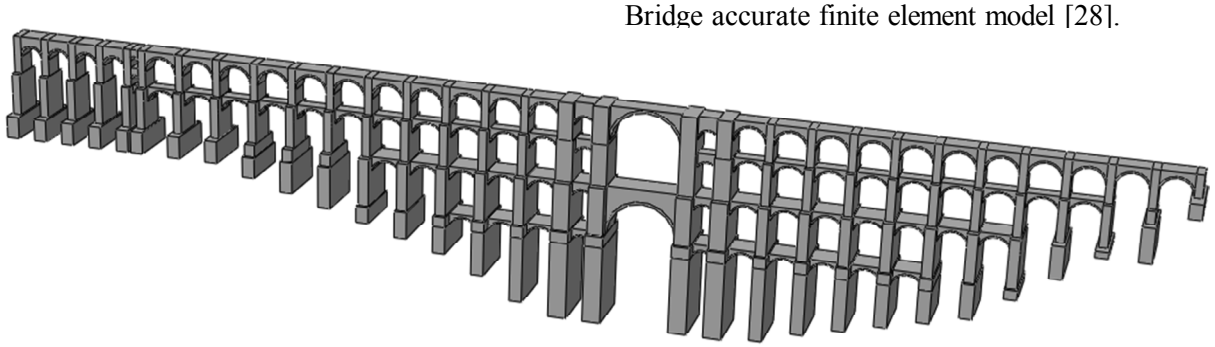

Figure 10. Finite element model of Goltzschtal Bridge.

Material properties of the accurate model are similar to those used in the simplified model. Springs that are modelled at two end walls of bridge, simulate the stiffness of walls backfills. Fill materials in various stories of bridge are simulated by low elastic modulus solid with real density.

Dynamic implicit analysis method is used for structural analysis of the bridge under seven selected records mentioned in Table (5). In accordance to complicated geometry of the bridge and for acceleration of solution procedure, four node linear tetrahedron element type is selected for structural meshing. The average values of $\frac{EQ}{DL}$ for axial forces in various sections of piers and arches of the bridge resulted from dynamic analysis for seven selected records have been shown in Table (6).

The situation of sections has been shown in Figure (11). The results obtained from dynamic analysis of simplified and accurate model under the near-field records are compared through Figure (12). This Figure shows that piers average values of $\frac{EQ}{DL}$ ratios in simplified model are in accordance with the ratios obtained for accurate model but differ excessively in the arches of two models, For the reason that in the simplified model the represented $\frac{EQ}{DL}$ ratio relates to all points located on sloped ceiling beam and is constant in the whole length of beam but in the accurate model represented $\frac{EQ}{DL}$ ratio relates to one special section of arch and varies in different sections of arch. These results show that the effects of vertical component of the near-field ground motions are noticeable in

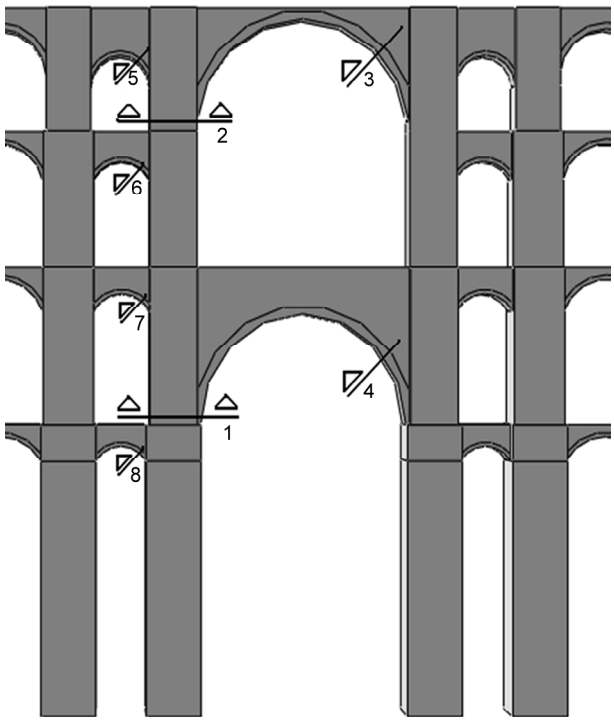

Figure 11. Situation of control sections.

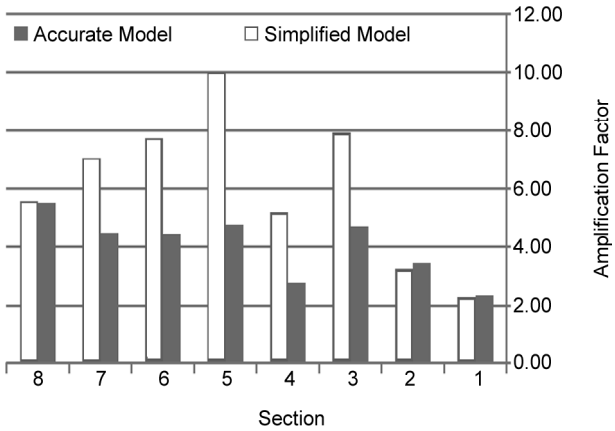

Figure 12. Dynamic analysis results of accurate and simplified model for far-field records.

Table 6. Average value of $\frac{EQ}{DL}$ in various sections of the bridge.

Average	Near-Field Amplification Factors							Section
	San Fernando	Manjil	Imperial Valley	Gazli	Northridge	Bam	Tabas	
2.34	3.14	1.9	2.35	2.3	2.985	1.82	1.86	1
3.43	3.86	2.85	3.77	3.83	4.335	2.82	2.55	2
4.73	5.24	3.47	5.37	4.37	5.9	5.16	3.57	3
2.78	4.08	2.75	2.72	2.47	2.67	2.35	2.41	4
4.77	5.02	3.62	5.9	6.49	5.04	3.58	3.71	5
4.47	3.55	3.05	5.68	5.9	5.54	3.59	3.96	6
4.50	5.8	3.39	6.18	4.33	5.08	3.46	3.25	7
5.50	7.97	5.72	4.28	5.1	6.5	4.99	3.96	8

Table 7. Specifications of 7 selected far field records.

Event Name	Station	Magnitude	PGA (g)	R (km)
Chi - Chi	TCU 095	7.62	0.26	52
Wither Narrow	Tarzana-cedar Hill	5.99	0.234	47.43
Morgan Hill	Hollister Differential Array #3	6.19	0.244	30.4
NorthRidge-01	LA-West Moreland	6.69	0.096	30.76
Tabas	Bajestan	7.35	0.03	119.77
Bam	Lalezar	6.6	0.008	155.46
Loma-Prieta	Berkeley LBL	6.93	0.834	33

structural elements of bridge.

Besides, for comparison of near-field and far-field earthquakes effects, seven far-field records are gathered from PEER NGA and accurate finite element model is analysed under these selected records. Table (7) shows the specifications of seven selected far-field records. Figure (13) shows the comparison between the average values of axial force $\frac{EQ}{DL}$ ratio resulted from dynamic analysis for selected far-field records and those obtained for near-field records.

In order to investigate the frequency content of responses in simplified and accurate model, time history of piers axial force responses in two different sections of a pier (Base and Section 5 according to Figure 11) extracted from nonlinear time history analysis of two models are plotted in Figures (14) and (15).

These Figures denote a good agreement of frequency content of responses in two models. In addition, the maximum value of $\frac{EQ}{DL}$ in section 1 of

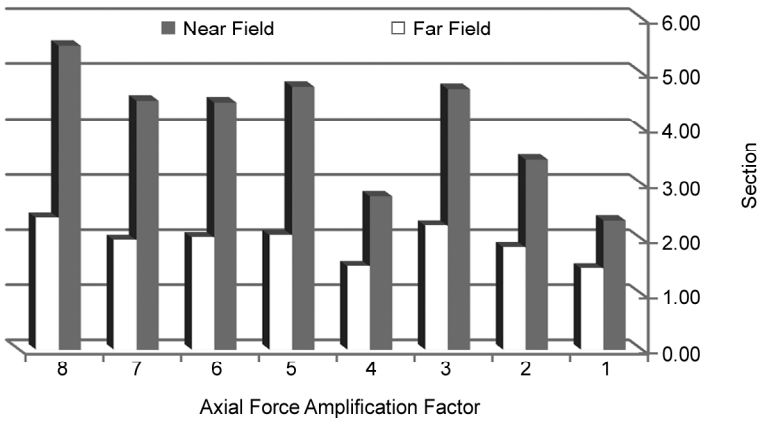

Figure 13. Dynamic analysis of accurate model results for far-field and near-field records.

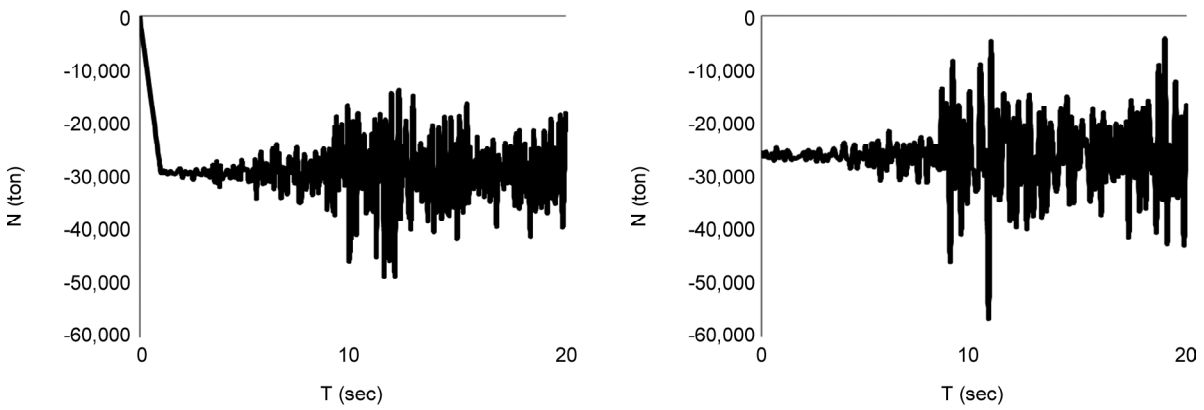

Figure 14. Time history of axial force responses in base of pier.

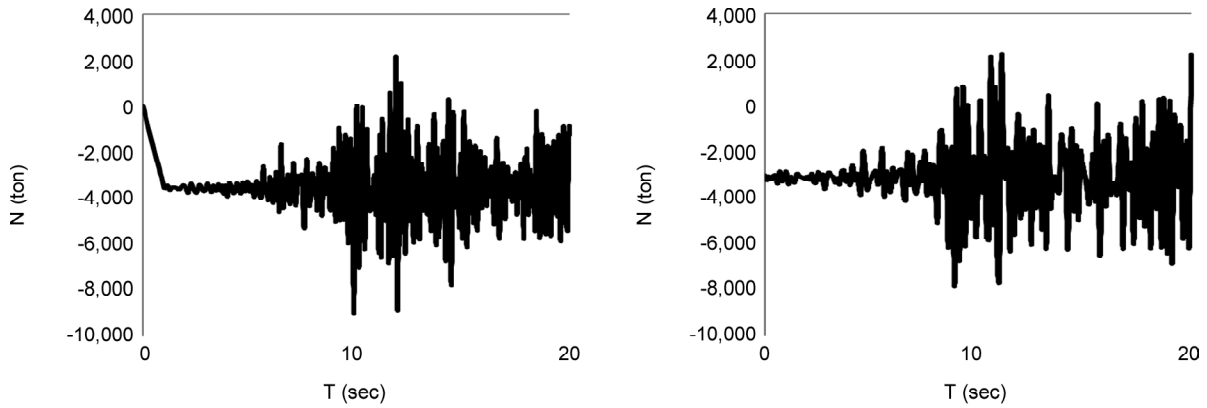

Figure 15. Time history of axial force responses in section 5 of pier.

pier (according to Figure 8) is compared with vertical component response spectrum value in $T = 0.25$ (period of bridge vertical vibration) for each earthquake and plotted in Figure (16). This figure shows the amplification of axial force due to the earthquake vertical component is considerable in earthquakes with high value of response spectrum.

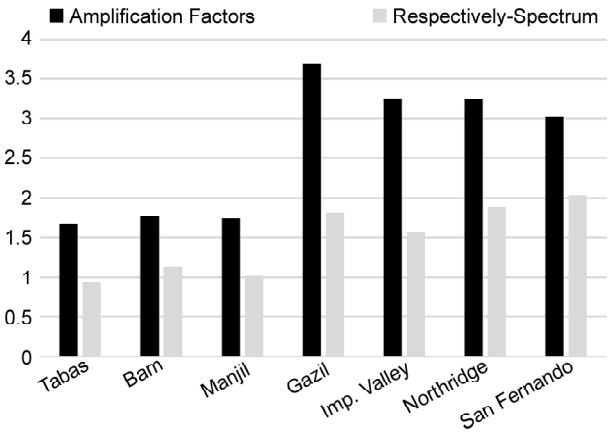

Figure 16. Variation of Axial force amplification factor and vertical component response spectrum value.

7. Nonlinear Time History Analysis

In the above-mentioned linear time history analysis, tensile and compression behaviours of masonry material are assumed to be equal, but tensile strength of such materials is negligible in practice. Thus, to investigate the effects of low tension strength of masonry materials on linear time history analysis results, nonlinear time history analysis is done on the segment consisting three central spans of Goltzschtal Bridge for vertical component of Tabas earthquake.

Concrete Damage Plasticity from ABAQUS Software material property options is selected for modelling the mechanical property of masonry material. Figure (17) shows the selected segment of Goltzschtal Bridge and Figure (18) shows stress strain curve used in the produced finite element model for compression and tensile loading respectively [29].

Piers axial force amplification factors extracted from nonlinear time history results represented in Table (8).

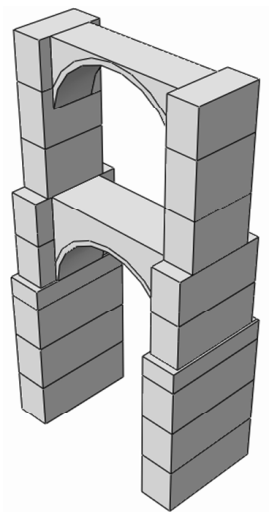

Figure 17. Segment of Goltzschtal Bridge.

Table 8. Piers axial forces amplification factors.

Position	Type of Analysis	
	Linear	Non Linear
EL 6152	3	2.6
EL 4395	2.5	2.3
EL 3030	2.28	2.10
EL 2350	2.10	1.92
EL 1879.70	2	1.90
EL 800	1.90	1.78

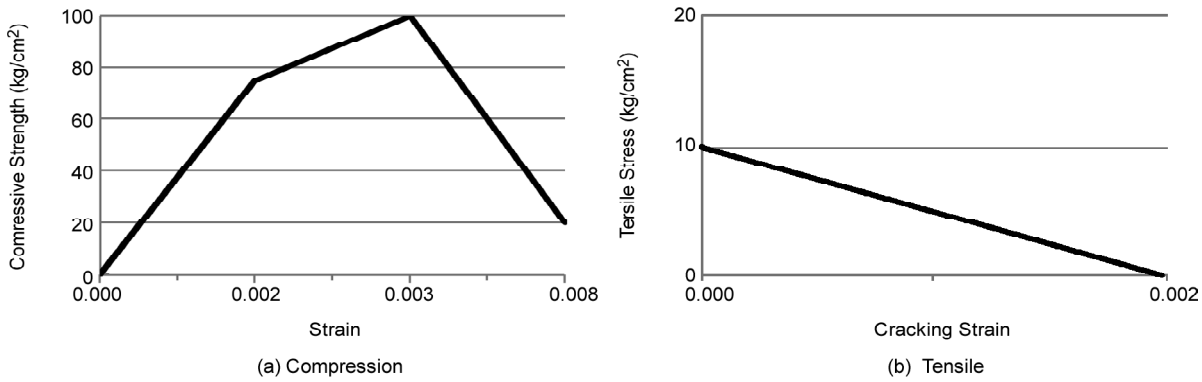

Figure 18. Stress strain curve used in finite element model.

Besides, for the verification of the results, a one-degree-of-freedom simplified model consisting cantilever bar and end concentrated mass is created in SAP2000 software environment. End mass and bar length of the simplified model are selected so that vertical vibration period can be equal in the simplified and accurate model. A gap element that eliminates axial tensile forces, are situated in the middle of the bar. Finally, nonlinear time history analysis is done on the simplified model under vertical component of Tabas earthquake. Figure (19) shows a view of simplified model and Table (9) presents axial forces amplification factor extracted from nonlinear time history results for simplified model with and without gap element.

Figure 19. A view of simplified one-degree-of-freedom model.

Table 9. Simplified model axial force amplification factor.

Type of Model	Bar Axial Forces Amplification Factor
With Gap Element	6.279
Without Gap Element	6.095

8. Conclusion

In this study, a simplified FE model of the world's largest brick bridge has been created and analysed under seven selected records. The results of nonlinear time history analysis have been represented as a ratio computed by dividing average values resulted based on applying three components of earthquake simultaneously for seven selected records to dead load responses of elements.

As mentioned earlier, because of geometrical shape and mechanical properties, masonry arch bridges have lower natural periods of vertical vibration and large amount of bridges modal mass is concentrated at low period regions (great peak region in response spectrum of vertical component in the near fault earthquakes) and as expectation, vertical ground motions effect are considerable in the elements of masonry arch bridges. For verification of the simplified model of dynamic analysis results, bridge's accurate finite element model is created, and time history dynamic analysis results are compared for simplified and accurate model. Comparing and reviewing axial force responses of Goltzschtal Bridge for seven selected near-field records in simplified and accurate models show that:

- Applying vertical component of near-field earthquakes increase the axial force in key structural elements excessively.
- Minimum values of $\frac{EQ}{DL}$ ratio for axial force responses are being observed in the piers of bridge that vary between 2.57 and 3.6. Maximum increase for the piers axial forces occurs in upper stories and minimum one occurs in the lower stories.
- Maximum values of the $\frac{EQ}{DL}$ ratio for axial force

responses are observing in the minor arches of bridge that vary between 6.23 and 9.16. Maximum increase for the minor arches axial forces occurs in the lower stories and minimum one occurs in the upper stories.

- Ratio of the $\frac{EQ}{DL}$ for axial force responses of major central arches lies between above-mentioned limits and varies between 5.19 and 7.52.
- Amount of increase in the arches axial forces have reverse relationship by span-length of arches.
- In the arches closer to bridge central axes, maximum increase in axial forces occurs in the upper stories but in arches far from bridge central axes, maximum increase occurs in the lower stories.
- Accurate model's dynamic analysis results are in accordance to those obtained from simplified model dynamic analysis.
- Average values of axial force the $\frac{EQ}{DL}$ ratio resulted from dynamic analysis under selected near-field records are greater in comparison to those obtained from far-field records.
- Because maximum tensile stresses in the piers are less than allowable tensile stresses and based on above-mentioned results, it is concluded that axial forces amplification factors are nearly equal for nonlinear and linear time history analysis and thus linear time history analysis results can be used to study the effects of vertical ground motions on axial force variation in bridge piers.

References

1. Newmark, N.M. and Hall, W.J. (1978) *Development of Criteria for Seismic Review of Selected Nuclear Power Plants*. NUREG/CR-0098, Nuclear Regulatory Commission.

2. Silva, W.J. (1997) Characteristics of vertical ground motions for application to engineering design. *Proc., FHWA/NCEER Workshop on the National Representation of Seismic Ground Motion for New and Existing Highway Facilities*, Tech. Rep. No. NCEER 97 0010, National Centre for earthquake engineering research, state Univ. of New York at buffalo, N.Y., 205-252.

3. Button, M.R., Cronin, C.J., and Mayes, R.L. (2002) Effect of vertical motions on seismic response of highway bridges. *Journal of Structural Engineering*, **128**, 1551-1564, DOI: 10.1061/~ASCE!0733-9445~2002!128:12~1551!.

4. Saadeghvaziri, M.A. and Foutch, D.A. (1998) Dynamic behavior of R/C high way bridges under the combined effect of vertical and horizontal earthquake motions. *J. Earthquake Eng. Struct. Dyn.*, **20**, 535-549, DOI: 10.1002/eqe.4290200604.

5. Yu, C.P., Broekhuizen, D.S., Roesset, J.M., Breen, J.E., and Kreger, M.E. (1997) Effect of vertical ground motion on bridge deck response. *Proc. Workshop on Earthquake Engineering Frontiers in Transportation Facilities*, Tech. Rep. No. NCEER-97-0005, National Center for Earthquake Engineering Research, State Univ. of New York at Buffalo, N.Y., 249-263

6. Broekhuizen, D.S. (1996) *Effects of Vertical Acceleration on Prestressed Concrete Bridges*. M.Sc. Thesis, Univ. of Texas at Austin, Tex.

7. Yu, C.P. (1996) *Effect of Vertical Earthquake Components on Bridge Responses*. Ph.D. Thesis, Univ. of Texas at Austin, Tex.

8. Gloyd, S. (1997) Design of ordinary bridges for vertical seismic acceleration. *Proc. FHWA/NCEER Workshop on the National Representation of Seismic Ground Motion for New and Existing Highway Facilities*, Tech. Rep. No. NCEER-97-0010, National Center for Earthquake Engineering Research, State Univ. of New York at Buffalo, N.Y., 277-290.

9. Sheng, L.H. and Kunnath, S.(2008) Effect of vertical acceleration on highway bridges. *Fourth US-Taiwan Bridge Engineering Workshop*, Princeton, Newjercey.

10. Kunnath, S.K., Abrahamson, N., Chai, Y.H., Erduran, E., and Yilmaz, Z. (2008) *Development of Guidelines for Incorporation of Vertical Ground Motion in Seismic Design of Highway Bridges*. A Technical Report Submitted to the California Department of Transportation under Contract 59A0434.

11. Hosseinzadeh, N.A. (2008) Vertical Component effect of Earthquake in seismic performance of

reinforced concrete bridges piers. *14th Conf. on Earthquake Engineering*, Beijing, China.

12. Armstrong, D.M., Sibbald, A., Fairfield, C.A., and Forde, M.C. (1995) Modal analysis for masonry arch bridge spandrell wall separation identification. *NDT&E International,* **28**(6), 377-386, DOI: 10.1016/0963-8695(95)00048-8.

13. Brencich, A. and Sabia, D. (2008) Experimental identification of multi-span masonry bridge: The Tanaro Bridge. *Construction and Building Materials*, **22**, 2087-2099, DOI:10.1016/j.conbuildmat.2007.07.031.

14. Bayraktar, A., Altunisik, A.C., Birinci, F., Sevim, B., and Türker, T. (2010) Finite-element analysis and vibration testing of a two-span masonry arch bridge. *Journal of Performance of Constructed Facilities*, **24**, 46-52, DOI: 10.1061/_ASCE_CF.1943-5509.0000060.

15. Caglayan, B.O., Ozakgul, K., Tezer, O., and Uzgider, E. (2011) Evaluation of a steel railway bridge for dynamic and seismic loads. *Journal of Constructional Steel Research*, **67**(8), 1198-1211, DOI:10.1016/j.jcsr.2011.02.013.

16. Yazdani, M., and Marefat, M.S. (2012) Evaluation of damping in unreinforced concrete arch bridges based on dynamic analysis. *Second International Conference on Acoustic and Vibration*, Tehran, Iran.

17. Pela, L., Aprile, A., and Benedetti, A. (2013) Comparison of seismic assessment for masonry arch bridges. *Construction and Building Materials*, **38**, 381-394, DOI:10.1016j.conbuildmat.2012.08.046.

18. Islamic Rep of Iran , Ministry of Roads and Transportation, Deputy of Training; Research and Information Technology (2008) *Road and Railway Bridges Seismic Resistant Design Code*.

19. CALTRANS (2010) *Seismic Design Criteria, Version 1.6*.

20. EuroCode 8 (2003) *Design of Structures for Earthquake Resistance, General Rules, Seismic Actions and Rules for Buildings*.

21. AASHTO (2012) *LRFD Bridge Design Specifications*. Washington, D.C.

22. AASHTO (1999) *Guide Specification for Design and Construction of Segmental Concrete Bridges*. Washington, D.C.

23. AASHTO (1996) *Standard Specification for Highway Bridges*. 16th Ed., Washington, D.C.

24. ASCE /SEI 7-10 (2013) *Minimum Design Loads for Buildings and Other Structures*.

25. ICC IBC (2012) *International Building Code*.

26. Uniform Building Code 97.

27. Wikipedia, the Free Encyclopedia, Goltzsch viaduct.

28. Sap2000 Ultimate 16.0.0, Structural Analysis Program, Manual.

29. Abaqus/CAE, Version 6.13, Structural Analysis Program.

30. Elmenshavi, A.S., Sorour, M., Mofti, A., and Jaeger, L.G. (2010) Damping mechanism and damping ratios in vibrating unreinforced stone masonry. *Journal of Engineering Structures*, **32**, 3269-3278, DOI: 10.1016/j.engstruct.2010.06.016.

31. Islami, K. (2013) *System Identification and Structural Health Monitoring of Bridge Structures*. Ph.D. Thesis, University of Padua, Italy.

32. Caglayan, B.O., Ozakgul, K., and Tezer, O. (2012) Assessment of a concrete arch bridge using static and dynamic load tests. *Journal of Structural Engineering and Mechanics*, **41**(1), 83-94.

33. Kaushik, H.B., Rai, D.C., and Jain, S.K. (2007) Uniaxial compressive stress-strain model for clay brick masonry. *Current Science*, **92**(4), 497-501.